International Journal of Solids and Structures 46 (2009) 2186–2200

Contents lists available at ScienceDirect

International Journal of Solids and Structures

journal homepage: www.elsevier.com/locate/ijsolstr

A moderate deflection composite helicopter rotor blade model with an improved cross-sectional analysis

Peretz P. Friedmann [a,*], Bryan Glaz [a], Rafael Palacios [b]

[a] Department of Aerospace Engineering, University of Michigan, 1320 Beal Avenue, 3001 FXB, Ann Arbor, MI 48109, USA
[b] Department of Aeronautics, Imperial College London, London SW7 2AZ, UK

ARTICLE INFO

Article history:
Received 3 March 2008
Received in revised form 29 August 2008
Available online 26 September 2008

Keywords:
Composite beams
Helicopter rotor blades
VABS

ABSTRACT

The compatibility between a composite beam cross-sectional analysis based on the variational asymptotic approach, and a helicopter rotor blade model which is part of a comprehensive rotorcraft analysis code is examined. It was found that the finite element cross-sectional analysis code VABS can be combined with a moderate deflection rotor blade model in spite of the differences between the formulations. The new YF/VABS rotor blade model accounts for arbitrary cross-sectional warping, in-plane stresses, and moderate deflections. The YF/VABS composite rotor blade model was validated against experimental data and various rotor blade analyses by examining displacements and stresses under static loads, as well as aeroelastic stability of a composite rotor blade in hover, and forward flight vibratory hubloads of a four bladed composite rotor.

1. Introduction

Accurate modeling of composite helicopter rotor blades is an important element in the development of comprehensive rotorcraft analysis codes. The composite rotor blade is a long and slender beam type structure subject to non-classical effects such as transverse shear deformation, geometric nonlinearities, cross-sectional warping, and elastic coupling due to material anisotropy. Over the past 25 years, significant advances have been made toward accurate modeling of composite blades with arbitrary cross-sectional geometry and material distribution. Particularly, Hodges and coworkers (Hodges, 2006; Danielson and Hodges, 1987; Hodges et al., 1992; Cesnik and Hodges, 1997; Popescu and Hodges, 1999) have developed a beam model which accounts for all of the non-classical effects mentioned above, while requiring significantly less computational effort than a direct three dimensional (3D) solution based on a nonlinear finite element discretization of the structure.

In the approach developed by Hodges et al., dimensional reduction of the 3D elasticity equations representing the slender structure is performed by means of an asymptotic approximation, which results in a 1D beam model. The dimensional reduction is based on the presence of a small parameter associated with the slender structure, namely the inverse of the blade's aspect ratio, which is used to split the 3D structural dynamic problem into two independent problems with different spatial scales: a 2D problem at the cross-section, and a 1D problem along the longitudinal dimension. The 1D problem defines the beam equations of motion, given in terms of 1D deformations – i.e. axial, bending, torsion, and shear deformation – under applied loads, while the solution of the 2D problem provides cross-sectional stiffness and inertia constants which depend on the material distribution and cross-sectional geometry. Since the 1D beam equations of motion are based on geometrically exact kinematics, the formulation is appropriate for large displacement analysis. The cross-sectional coefficients needed as inputs to the 1D beam solver come from the 2D finite element code VABS (variational asymptotic beam sectional analysis),

* Corresponding author. Tel.: +1 734 763 2354; fax: +1 734 763 0578.
E-mail address: peretzf@umich.edu (P.P. Friedmann).

0020-7683/$ - see front matter © 2008 Elsevier Ltd. All rights reserved.
doi:10.1016/j.ijsolstr.2008.09.017

which accounts for arbitrary in and out-of-plane cross-sectional warping. Although warping displacements are much smaller than the 1D beam deformations, accurate modeling of the warping is important since the stress field is a function of warping derivatives which may not be small (Hodges, 2006). The work by Hodges et al. represents the state of the art in computationally efficient structural modeling of a composite rotor blade. Detailed reviews of structural modeling of helicopter rotor blades can be found in Hodges (1990, 2006) and Jung et al. (1999). Note that a substantial body of research on geometrically exact beam theory exists. This research has been motivated by applications other than helicopter rotor blade modeling, e.g. Simo (1985), Simo and Vu-Quoc (1986), Bori and Merlini (1986), Cardona and Geradin (1988), Crisfield (1990), Simo et al. (1995), and Ibrahimbegovic et al. (1995). However, a detailed review of the subject is beyond the scope of this paper.

In parallel to the emphasis on the structural aspect of rotor blade modeling carried out by Hodges and his associates, research on other aspects which are equally important for comprehensive rotorcraft analysis, such as unsteady aerodynamics, active control of noise and vibration, global optimization of rotor blades for vibration reduction, and active/passive optimization for noise and vibration reduction, was conducted by Friedmann and coworkers (Myrtle and Friedmann, 2001; Patt et al., 2006; Glaz et al., 2008a,b). Other comprehensive rotorcraft analysis codes are discussed in Friedmann and Hodges (2003) and Friedmann (2004). The rotor blade analysis developed by Friedmann and his associates has a composite blade modeling capability described in Yuan and Friedmann (1995, 1998) and Kosmatka (1986). In this composite blade model, higher order terms associated with the strain–displacement relations are neglected using an ordering scheme, which results in a 1D kinematical formulation appropriate for moderate deflection analysis only. In the moderate deflection analysis, blade displacements up to 10–15% of the blade radius can be accurately modeled. The moderate deflection simplification is justified for composite helicopter rotor blade analysis since rotor blades are designed from low stress and long-cycle fatigue considerations, while large displacements imply larger strains and thus higher stresses and increased fatigue. Therefore, it is unlikely that a well designed rotor blade will be subject to large displacements.

Although the cross-sectional analysis utilized in Yuan and Friedmann (1995, 1998) and Kosmatka (1986) can account for arbitrary cross-sectional geometries and material distributions, in-plane stresses and warping were neglected. In VABS, the in-plane stresses are not neglected since it has been shown that the uniaxial stress assumption can lead to significant errors in the torsional rigidity for some composite cross-sections (Yu et al., 2002b). Furthermore, the out-of-plane warping deformation associated with the structural model from Yuan and Friedmann (1995, 1998) and Kosmatka (1986) is based on the St. Venant solution of a tip-loaded prismatic beam, as opposed to the more general warping displacements modeled in VABS. Another advantage of VABS is that the variational-asymptotic approach provides a powerful tool for extending basic theory, e.g. the solution of the coupled electroelastic beam problem, which is applicable to rotor blades with embedded piezocomposites, and the treatment of non-classical cross-sectional deformations associated with rotor blades with adaptive airfoils (Palacios and Cesnik, 2005, 2008). In both cases, however, the 1D beam equations needed to be modified to account for the additional effects.

Clearly, it is desirable to upgrade the blade model in the Friedmann et al. analysis code with VABS. Although VABS was designed to be used with the geometrically exact formulation described in Hodges (2006), it has been used to calculate the cross-sectional properties needed as inputs for other rotorcraft analysis codes (Hodges et al., 2007; Murugan et al., 2007). However, there are two differences associated with the blade model developed by Yuan and Friedmann and the other models with which VABS has been coupled: (1) the amplitude of the out-of-plane warping is represented as a spanwise degree of freedom in the Yuan and Friedmann (YF) model and (2) there are cross-sectional constants associated with the YF model which are not computed in the VABS formulation. Furthermore, the justification for using VABS, as well as the capabilities and limitations of the resulting blade models, have not been examined in the existing literature.

The overall objectives of this paper are: (a) demonstrate that VABS can be used as the cross-sectional analysis associated with the YF blade model despite the differences between the formulations and without extensive modification to the numerous underlying subroutines associated with comprehensive rotorcraft analysis codes, and (b) to provide a clear methodology and complete description of the implications of incorporating VABS into existing helicopter comprehensive analysis codes. The YF blade model combined with VABS coefficients is designated YF/VABS, and is validated in this paper by:

(1) Demonstrating that displacement and stresses calculated by the YF/VABS compare well with experimental results and results generated by a geometrically exact beam model developed for use with VABS, as long as displacements are in the moderate deflection regime.
(2) Comparing the YF/VABS model with other rotorcraft analyses for several helicopter applications such as composite rotor blade aeroelastic stability analysis in hover and computation of 4/rev forward flight vibratory hub shears and moments of a four bladed composite rotor.

2. Comparison of cross-sectional analyses

In order to determine the compatibility between the cross-sectional properties calculated by VABS and those needed as inputs to the YF blade model, it is useful to understand the similarities and differences between the two formulations. Therefore, this section provides comparisons between the strain relations, constitutive relations, the resulting strain energy

relations, and the kinetic energy relations associated with the two formulations. The strain and kinetic energy relations are functions of the cross-sectional coefficients associated with each model.

2.1. Strain relations

Consider a beam idealized as a reference line, with a cross-section depicted in Fig. 1. A coordinate system parallel to the orthogonal unit vectors $\mathbf{b}_i$ for $i = 1, 2, 3$ is fixed at each point along the undeformed reference line, where $\mathbf{b}_1$ is tangent to the reference line and $\mathbf{b}_2, \mathbf{b}_3$ are orthogonal to $\mathbf{b}_1$. The coordinates x_2 and x_3 correspond to the $\mathbf{b}_2, \mathbf{b}_3$ unit vectors respectively, while x_1 denotes the axial location of the cross-section.

From Yuan and Friedmann (1995), the non-zero components of the strain tensor in the $\mathbf{b}_i$ system associated with the YF blade model are given by

$$\Gamma_{11}^{(Y)} = \gamma_{11} + w_{1,1}^{(Y)} + k_1\left(x_3 w_{1,2}^{(Y)} - x_2 w_{1,3}^{(Y)}\right) - x_2(\bar{\kappa}_3 - 2\gamma_{12,1} + 2k_1\gamma_{13}) - x_3(-\bar{\kappa}_2 - 2\gamma_{13,1} - 2k_1\gamma_{12}) + \frac{1}{2}(x_2^2 + x_3^2)\bar{\kappa}_1^2, \tag{1}$$

$$2\Gamma_{12}^{(Y)} = 2\gamma_{12} + w_{1,2}^{(Y)} - x_3\bar{\kappa}_1, \tag{2}$$

$$2\Gamma_{13}^{(Y)} = 2\gamma_{13} + w_{1,3}^{(Y)} + x_2\bar{\kappa}_1, \tag{3}$$

where the (Y) superscript denotes association with the YF blade model and $(\,)_{,i}$ denotes a derivative with respect to the x_i coordinate. In Eqs. (1)–(3), the 1D axial and shear strain measures at the reference line, which are functions of the x_1 coordinate only, are given by γ_{11}, γ_{12}, and γ_{13}, respectively. The initial twist is denoted by k_1. The out-of-plane warping displacements w_1 are functions of x_1, x_2, and x_3. In the YF model,

$$w_1^{(Y)}(x_1, x_2, x_3) = \alpha(x_1)\Psi(x_2, x_3), \tag{4}$$

where $\alpha(x_1)$ is the unknown 1D warping amplitude and $\Psi(x_2, x_3)$ is the 2D warping shape function. The warping shape functions are based on the St. Venant solution of a tip-loaded prismatic beam (Kosmatka, 1986) and thus are known for a given cross-section.

The 1D "moment strains" (Hodges, 2006), $\bar{\kappa}_i$, are with respect to a coordinate system parallel to the $\mathbf{T}_i$ basis vectors shown in Fig. 2 and represent the differences between the deformed and initial states of the twist and bending curvatures. The elastic twist is given by $\bar{\kappa}_1$, while $\bar{\kappa}_2$ and $\bar{\kappa}_3$ are the moment strains corresponding to bending. Since the helicopter rotor blade is assumed to have no initial curvature in the YF model, the bending moment strains are equal to the deformed bending curvatures.

In the VABS formulation, the moment strains are written with respect to the $\mathbf{B}_i$ coordinate system and denoted by κ_i. The $\mathbf{T}_i$ and $\mathbf{B}_i$ systems differ due to transverse shear deformation since $\mathbf{T}_1$ is tangent to the deformed reference line, while $\mathbf{B}_1$ is normal to the deformed cross-section. With the assumption of no initial bending curvature, the elastic twist and the deformed bending curvatures in the $\mathbf{T}_i$ system are transformed to the $\mathbf{B}_i$ coordinate system by (Yu et al., 2002a)

$$\bar{\kappa}_1 = \kappa_1, \tag{5}$$

$$\bar{\kappa}_2 = \kappa_2 - 2\gamma_{13,1} - 2k_1\gamma_{12}, \tag{6}$$

$$\bar{\kappa}_3 = \kappa_3 + 2\gamma_{12,1} - 2k_1\gamma_{13}. \tag{7}$$

The YF strain relations can be rewritten in a form which is consistent with the VABS formulation by substituting Eqs. (5)–(7) into Eqs. (1)–(3), resulting in

$$\Gamma_{11}^{(Y)} = \gamma_{11} + w_{1,1}^{(Y)} + k_1\left(x_3 w_{1,2}^{(Y)} - x_2 w_{1,3}^{(Y)}\right) - x_2\kappa_3 + x_3\kappa_2 + \frac{1}{2}(x_2^2 + x_3^2)\kappa_1^2, \tag{8}$$

$$2\Gamma_{12}^{(Y)} = 2\gamma_{12} + w_{1,2}^{(Y)} - x_3\kappa_1, \tag{9}$$

$$2\Gamma_{13}^{(Y)} = 2\gamma_{13} + w_{1,3}^{(Y)} + x_2\kappa_1. \tag{10}$$

Note that $\Gamma_{22}^{(Y)} = \Gamma_{23}^{(Y)} = \Gamma_{33}^{(Y)} = 0$ since in-plane warping is neglected in the YF model.

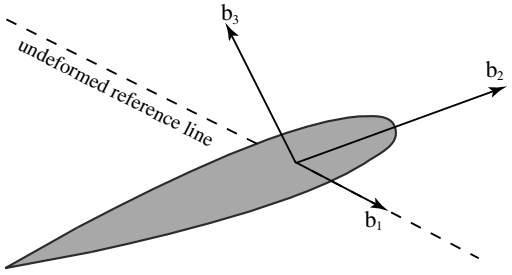

Fig. 1. Undeformed coordinate system.

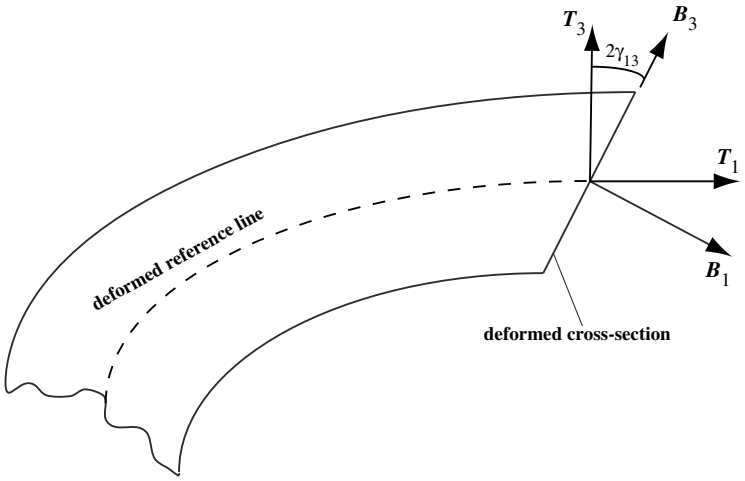

Fig. 2. Coordinate systems which differ due to transverse shear deformations.

From Hodges (2006), the strain relations corresponding to VABS' "generalized Timoshenko model" with the "trapeze effect" are given by

$$\Gamma_{11}^{(V)} = \gamma_{11} + w_{1,1}^{(V)} + k_1\left(x_3 w_{1,2}^{(V)} - x_2 w_{1,3}^{(V)}\right) - x_2\kappa_3 + x_3\kappa_2 + \frac{1}{2}\left(x_2^2 + x_3^2\right)\kappa_1^2 + \text{H.O.T.}, \tag{11}$$

$$2\Gamma_{12}^{(V)} = 2\gamma_{12} + w_{1,2}^{(V)} - x_3\kappa_1 + f_{12}\left(w_2^{(V)}, w_3^{(V)}\right) + \text{H.O.T.}, \tag{12}$$

$$2\Gamma_{13}^{(V)} = 2\gamma_{13} + w_{1,3}^{(V)} + x_2\kappa_1 + f_{13}\left(w_2^{(V)}, w_3^{(V)}\right) + \text{H.O.T.}, \tag{13}$$

$$\Gamma_{22}^{(V)} = f_{22}\left(w_2^{(V)}\right) + \text{H.O.T.} \neq 0, \quad \Gamma_{23}^{(V)} = f_{23}\left(w_2^{(V)}, w_3^{(V)}\right) + \text{H.O.T.} \neq 0,$$

$$\Gamma_{33}^{(V)} = f_{33}\left(w_3^{(V)}\right) + \text{H.O.T.} \neq 0, \tag{14}$$

where the (V) superscript denotes association with VABS, f_{ij} represent the contributions from the in-plane warping to the strain field, and H.O.T. refers to higher order terms which are present in the VABS formulation but are not accounted for in the YF strain relations.

In VABS, the warping displacements are discretized over the cross-section using the finite element approach. The VABS warping displacements can be written as

$$w_i^{(V)}(x_1, x_2, x_3) = S_{ij}(x_2, x_3)V_j(x_1), \quad i = 1, 2, 3 \text{ and } j = 1, 2, \ldots, N_V. \tag{15}$$

In Eq. (15), S_{ij} are 2D finite element shape functions, V_j are the nodal values of the warping displacement over the cross-section, and N_V is the number of nodal degrees of freedom. In contrast to the YF formulation, the VABS warping displacements are not assumed to be in the shape of the St. Venant warping function $\Psi(x_2, x_3)$. Since the shape of the warping is not assumed, VABS treats warping displacements in a more general manner than the YF model.

The H.O.T.'s in Eqs. (11)–(13) consist of nonlinearities in the 1D strain measures, such as γ_{11}^2 and $\kappa_2\kappa_3$ for example, and couplings between the warping displacements and the 1D strain measures. Such H.O.T.'s were neglected in the derivation of the YF strain equations. However, $\frac{1}{2}(x_2^2 + x_3^2)\kappa_1^2$ was retained in the YF formulation since it accounts for a higher order extension-torsion coupling known as the "trapeze effect", which is known to be important for helicopter rotor blade modeling due to the large centrifugal forces.

From comparison of Eqs. (8)–(10) with Eqs. (11)–(14), it is clear that there are three differences in the strain relations associated with the VABS and YF formulations:

(1) VABS treats out-of-plane warping in a more general manner, thus $w_1^{(V)} \neq w_1^{(Y)}$.
(2) The effects of in-plane warping on the strain field are accounted for in VABS.
(3) VABS includes higher order couplings between the 1D strain measures, and coupling between the 1D strain measures and warping displacements, which are neglected in the YF formulation.

2.2. Constitutive relations

The constitutive relation for an anisotropic material is given by

$$\boldsymbol{\sigma}^{(V)} = \mathbf{D}\boldsymbol{\Gamma}^{(V)}, \tag{16}$$

where

$$\boldsymbol{\sigma}^{(V)} = [\,\sigma_{11} \quad \sigma_{12} \quad \sigma_{13} \quad \sigma_{22} \quad \sigma_{23} \quad \sigma_{33}\,]^{\mathrm{T}}, \tag{17}$$

$$\boldsymbol{\Gamma}^{(V)} = [\,\Gamma_{11} \quad 2\Gamma_{12} \quad 2\Gamma_{13} \quad \Gamma_{22} \quad 2\Gamma_{23} \quad \Gamma_{33}\,]^{\mathrm{T}}, \tag{18}$$

and $\mathbf{D}$ is the 6×6 symmetric compliance matrix. The VABS constitutive relation is based on Eq. (16). In contrast, the YF model employs the uniaxial stress assumption, i.e. $\sigma_{22} = \sigma_{23} = \sigma_{33} = 0$. After neglecting the in-plane stresses, the constitutive relation associated with the YF model is written as

$$\boldsymbol{\sigma}^{(Y)} = \mathbf{Q}\boldsymbol{\Gamma}^{(Y)}, \tag{19}$$

where

$$\boldsymbol{\sigma}^{(Y)} = [\,\sigma_{11} \quad \sigma_{12} \quad \sigma_{13}\,]^{\mathrm{T}}, \tag{20}$$

$$\boldsymbol{\Gamma}^{(Y)} = [\,\Gamma_{11} \quad 2\Gamma_{12} \quad 2\Gamma_{13}\,]^{\mathrm{T}}, \tag{21}$$

and $\mathbf{Q}$ is a 3×3 symmetric matrix. Expressions for $\mathbf{Q}$ in terms of the $\mathbf{D}$ matrix's elements can be found in Yuan and Friedmann (1995). Although the uniaxial stress assumption was considered valid for composite thin-walled structures in Yuan and Friedmann (1995), it was demonstrated in Yu et al. (2002b) and Hodges (2006) that this simplification may lead to significant errors in the torsional rigidity of a thin-walled composite boxbeam. Therefore, while the uniaxial stress simplification may lead to acceptable results for some composite cross-sections, the only way to ensure correct results for all cases is to employ a formulation, such as the one associated with VABS, which does not neglect in-plane stresses.

2.3. Strain energy relations

The relation for strain energy, U, is

$$2U = \int_0^L \int_A \boldsymbol{\Gamma}^{\mathrm{T}}\boldsymbol{\sigma}\,\mathrm{d}A\,\mathrm{d}x_1, \tag{22}$$

where L is the length of the beam, and A is the cross-sectional area of the structural member. Substitution of Eqs. (4), (8), (9), (10), and (19) into Eq. (22) gives the strain energy associated with the YF model

$$2U^{(Y)} = \int_0^L \boldsymbol{\epsilon}_Y^{\mathrm{T}}\mathbf{Y}\boldsymbol{\epsilon}_Y\,\mathrm{d}x_1, \tag{23}$$

where

$$\boldsymbol{\epsilon}_Y = [\,\gamma_{11} \quad 2\gamma_{12} \quad 2\gamma_{13} \quad \kappa_1 \quad \kappa_2 \quad \kappa_3 \quad \kappa_1^2 \quad \alpha \quad \alpha_{,1}\,]^{\mathrm{T}} \tag{24}$$

and $\mathbf{Y}$ is a 9×9 symmetric matrix containing integrals over the cross-section. The elements of $\mathbf{Y}$ are needed as inputs for the YF model, and are computed by the 2D finite element cross-sectional analysis described in Kosmatka (1986). To facilitate a straight forward comparison with the VABS strain energy relation, Eq. (23) can be rewritten as

$$2U^{(Y)} = 2\int_0^L \left(u_1^{(Y)} + u_2^{(Y)} + u_\alpha^{(Y)}\right)\mathrm{d}x_1, \tag{25}$$

where

$$u_1^{(Y)} = \frac{1}{2}\begin{bmatrix}\gamma_{11}\\ 2\gamma_{12}\\ 2\gamma_{13}\\ \kappa_1\\ \kappa_2\\ \kappa_3\end{bmatrix}^{\mathrm{T}}\begin{bmatrix}Y_{11} & Y_{12} & Y_{13} & Y_{14} & Y_{15} & Y_{16}\\ Y_{12} & Y_{22} & Y_{23} & Y_{24} & Y_{25} & Y_{26}\\ Y_{13} & Y_{23} & Y_{33} & Y_{34} & Y_{35} & Y_{36}\\ Y_{14} & Y_{24} & Y_{34} & Y_{44} & Y_{45} & Y_{46}\\ Y_{15} & Y_{25} & Y_{35} & Y_{45} & Y_{55} & Y_{56}\\ Y_{16} & Y_{26} & Y_{36} & Y_{46} & Y_{56} & Y_{66}\end{bmatrix}\begin{bmatrix}\gamma_{11}\\ 2\gamma_{12}\\ 2\gamma_{13}\\ \kappa_1\\ \kappa_2\\ \kappa_3\end{bmatrix}, \tag{26}$$

$$u_2^{(Y)} = \kappa_1^2\left(Y_{17}\gamma_{11} + 2Y_{27}\gamma_{12} + 2Y_{37}\gamma_{13} + Y_{47}\kappa_1 + Y_{57}\kappa_2 + Y_{67}\kappa_3 + \frac{Y_{77}}{2}\kappa_1^2\right), \tag{27}$$

$$u_\alpha^{(Y)} = \begin{bmatrix}\alpha\\ \alpha_{,1}\end{bmatrix}\begin{bmatrix}Y_{18} & \dots & \frac{Y_{88}}{2} & Y_{89}\\ Y_{19} & \dots & Y_{89} & \frac{Y_{99}}{2}\end{bmatrix}\boldsymbol{\epsilon}_Y. \tag{28}$$

The VABS strain energy is a function of the following 1D parameters: γ_{11}, $2\gamma_{12}$, $2\gamma_{13}$, κ_1, κ_2, κ_3, and V_j, i.e.

$$2U^{(V)} = f(\gamma_{11}, 2\gamma_{12}, 2\gamma_{13}, \kappa_1, \kappa_2, \kappa_3, V_j). \tag{29}$$

From Eqs. (23) and (24), it is clear that $U^{(Y)}$ is similar in form to $U^{(V)}$ in the sense that $U^{(Y)}$ is a function of γ_{11}, $2\gamma_{12}$, $2\gamma_{13}$, κ_1, κ_2, κ_3, and the 1D warping variable α. However, in VABS the variational asymptotic method is applied in order to obtain an approximation of $U^{(V)}$ which is *not* a function of the 1D warping variables, i.e.

$$2U^{(V)} \cong 2\widetilde{U}^{(V)} = \tilde{f}(\gamma_{11}, 2\gamma_{12}, 2\gamma_{13}, \kappa_1, \kappa_2, \kappa_3), \tag{30}$$

where $\widetilde{U}^{(V)}$ and $\tilde{f}$ are the approximations of $U^{(V)}$. The approximation of $U^{(V)}$ is obtained by minimizing the strain energy with respect to warping, which results in *warping recovery relations* for the nodal displacements V_j. The warping recovery relations are functions of the 1D strain measures, γ_{11}, $2\gamma_{12}$, $2\gamma_{13}$, κ_1, κ_2, and κ_3.

In the original VABS strain energy $U^{(V)}$, the contribution due to warping is associated with the cross-sectional parameters multiplying V_j. However, in the approximate VABS strain energy, $\widetilde{U}^{(V)}$, the contributions from warping are accounted for by a new set of cross-sectional parameters which multiply γ_{11}, $2\gamma_{12}$, $2\gamma_{13}$, κ_1, κ_2, and κ_3. Therefore, by approximating $U^{(V)}$ with $\widetilde{U}^{(V)}$, the strain energy associated with warping displacements is accounted for by the terms multiplying the 1D strain measures. Details on the application of the variational asymptotic method and the resulting expressions are given in Chapter 4 of Hodges (2006). From Hodges (2006), the VABS strain energy is given by

$$2\widetilde{U}^{(V)} = \int_0^L \begin{bmatrix} \gamma_{11} \\ 2\gamma_{12} \\ 2\gamma_{13} \\ \kappa_1 \\ \kappa_2 \\ \kappa_3 \end{bmatrix}^{\mathrm{T}} \begin{bmatrix} H_{11} & H_{12} & H_{13} & H_{14} & H_{15} & H_{16} \\ H_{12} & H_{22} & H_{23} & H_{24} & H_{25} & H_{26} \\ H_{13} & H_{23} & H_{33} & H_{34} & H_{35} & H_{36} \\ H_{14} & H_{24} & H_{34} & H_{44} & H_{45} & H_{46} \\ H_{15} & H_{25} & H_{35} & H_{45} & H_{55} & H_{56} \\ H_{16} & H_{26} & H_{36} & H_{46} & H_{56} & H_{66} \end{bmatrix} \begin{bmatrix} \gamma_{11} \\ 2\gamma_{12} \\ 2\gamma_{13} \\ \kappa_1 \\ \kappa_2 \\ \kappa_3 \end{bmatrix} \mathrm{d}x_1 + 2\int_0^L \begin{bmatrix} \gamma_{11} \\ \kappa_1 \\ \kappa_2 \\ \kappa_3 \end{bmatrix}^{\mathrm{T}} (\gamma_{11}\mathbf{A} + \kappa_1\mathbf{B} + \kappa_2\mathbf{C} + \kappa_3\mathbf{D}) \begin{bmatrix} \gamma_{11} \\ \kappa_1 \\ \kappa_2 \\ \kappa_3 \end{bmatrix} \mathrm{d}x_1, \tag{31}$$

where **A**, **B**, **C**, and **D** are symmetric 4×4 matrices. Note that the strain energy terms associated with **A**, **B**, **C**, and **D** are higher order functions of the 1D strain measures than the terms associated with **H**. The **H**, **A**, **B**, **C**, and **D** matrices are output by VABS. In order to compare with $U^{(Y)}$, Eq. (31) can be rewritten as

$$2\widetilde{U}^{(V)} = 2\int_0^L \left(u_1^{(V)} + u_2^{(V)} + u_{\mathrm{H.O.T.}}^{(V)}\right)\mathrm{d}x_1, \tag{32}$$

where

$$u_1^{(V)} = \frac{1}{2} \begin{bmatrix} \gamma_{11} \\ 2\gamma_{12} \\ 2\gamma_{13} \\ \kappa_1 \\ \kappa_2 \\ \kappa_3 \end{bmatrix}^{\mathrm{T}} \begin{bmatrix} H_{11} & H_{12} & H_{13} & H_{14} & H_{15} & H_{16} \\ H_{12} & H_{22} & H_{23} & H_{24} & H_{25} & H_{26} \\ H_{13} & H_{23} & H_{33} & H_{34} & H_{35} & H_{36} \\ H_{14} & H_{24} & H_{34} & H_{44} & H_{45} & H_{46} \\ H_{15} & H_{25} & H_{35} & H_{45} & H_{55} & H_{56} \\ H_{16} & H_{26} & H_{36} & H_{46} & H_{56} & H_{66} \end{bmatrix} \begin{bmatrix} \gamma_{11} \\ 2\gamma_{12} \\ 2\gamma_{13} \\ \kappa_1 \\ \kappa_2 \\ \kappa_3 \end{bmatrix}, \tag{33}$$

$$u_2^{(V)} = \kappa_1^2[(A_{22} + 2B_{12})\gamma_{11} + B_{22}\kappa_1 + (2B_{23} + C_{22})\kappa_2 + (2B_{24} + D_{22})\kappa_3], \tag{34}$$

$$u_{\mathrm{H.O.T.}}^{(V)} = \begin{bmatrix} \gamma_{11} \\ \kappa_1 \\ \kappa_2 \\ \kappa_3 \end{bmatrix}^{\mathrm{T}} (\gamma_{11}\mathbf{A} + \kappa_1\mathbf{B} + \kappa_2\mathbf{C} + \kappa_3\mathbf{D}) \begin{bmatrix} \gamma_{11} \\ \kappa_1 \\ \kappa_2 \\ \kappa_3 \end{bmatrix} - u_2^{(V)}. \tag{35}$$

Using the strain energy relations given in Eqs. (25)–(28) for the YF formulation, and Eqs. (32)–(35) for VABS, a direct comparison of the cross-sectional parameters associated with both models can be made. The comparison is organized into three categories – (1) terms which are present in both model, (2) terms which are present in VABS' strain energy relation, but are not accounted for in the YF model, and (3) terms present in the YF model, but are not included in the VABS formulation.

2.3.1. Strain energy terms present in both models

A comparison of Eqs. (26) and (27) with Eqs. (33) and (34) shows that

$$Y_{ij} \Longleftrightarrow H_{ij} \quad \text{for } i,j = 1,\ldots,6, \tag{36}$$

$$Y_{17} \Longleftrightarrow A_{22} + 2B_{12}, \tag{37}$$

$$Y_{47} \Longleftrightarrow B_{22}, \tag{38}$$

$$Y_{57} \Longleftrightarrow 2B_{23} + C_{22}, \tag{39}$$

$$Y_{67} \Longleftrightarrow 2B_{24} + D_{22}. \tag{40}$$

In Eqs. (36)–(40), "⇔" denotes that the cross-sectional parameters multiply the same 1D strain measures. It is important to use "⇔" instead of "=" because the cross-sectional parameters will not be equal to one another in general. There are two reasons the cross-sectional parameters in Eqs. (36)–(40) will not be equal:

(1) In the constitutive relations associated with the YF model, the in-plane stresses are neglected; thus Eq. (19) is substituted into Eq. (22) in order to derive the strain energy relation. However, VABS does not make the uniaxial stress simplification. Therefore, the VABS strain energy relation is obtained by substituting Eq. (16) into Eq. (22).
(2) The 1D warping variables are eliminated from the VABS strain energy formulation, which results in $\widetilde{U}^{(V)}$. In effect, VABS accounts for the strain energy due to in and out-of-plane warping in the **H**, **A**, **B**, **C**, and **D** matrices, which multiply the 1D strain measures and are functions of S_{ij}. However, the warping strain energy in the YF model is retained in terms of the 1D out-of-plane warping amplitude α and the cross-sectional coefficients Y_{i8} and Y_{i9}, which are functions of Ψ.

2.3.2. Strain energy terms present in VABS, but not in the YF model

The higher order VABS strain energy terms, $u^{(V)}_{\text{H.O.T.}}$, are not accounted for in the YF model. The strain energy contribution from $u^{(V)}_{\text{H.O.T.}}$ is due to the H.O.T.'s retained in the VABS strain relations.

2.3.3. Strain energy terms present in the YF model, but not in VABS

A comparison of Eqs. (27) and (34) shows that VABS does not output cross-sectional coefficients which correspond to Y_{27}, Y_{37}, and Y_{77}. Such terms were neglected in the VABS strain energy formulation (Hodges, 2006). In addition, VABS does not calculate cross-sectional properties which correspond to the Y_{i8} and Y_{i9} terms present in $u^{(Y)}_{\alpha}$. Instead, VABS accounts for the strain energy due to warping within the **H**, **A**, **B**, **C**, and **D** matrices.

2.4. Kinetic energy relations

The kinetic energy cross-sectional properties calculated by VABS are given in Eqs. (41)–(46),

$$m \equiv \int\int_A \rho \, \mathrm{d}A, \tag{41}$$

$$m_{x_2} \equiv \int\int_A \rho x_2 \, \mathrm{d}A, \tag{42}$$

$$m_{x_3} \equiv \int\int_A \rho x_3 \, \mathrm{d}A, \tag{43}$$

$$I_{m_{22}} \equiv \int\int_A \rho x_3^2 \, \mathrm{d}A, \tag{44}$$

$$I_{m_{33}} \equiv \int\int_A \rho x_2^2 \, \mathrm{d}A, \tag{45}$$

$$I_{m_{23}} \equiv \int\int_A \rho x_2 x_3 \, \mathrm{d}A, \tag{46}$$

where ρ is the material density. The YF model requires the same kinetic energy cross-sectional parameters given by Eqs. (41)–(46) as inputs. In addition, the YF model also requires cross-sectional properties associated with the kinetic energy due to warping velocities (Yuan and Friedmann, 1995). Since warping velocity is neglected in the VABS formulation (Hodges, 2006), VABS will not output cross-sectional properties associated with kinetic energy due to warping.

3. The YF/VABS blade model

In Section 2, the similarities and differences between the two cross-sectional analyses were specified. This section provides a description of how the similarities can be used to couple VABS with the YF model, and justification for why the differences between the cross-sectional formulations do not prevent the coupling. The capabilities and limitations of the YF/VABS model will be described in terms of the cross-sectional analysis, the solution of the 1D beam displacements, and recovery of cross-sectional warping displacements and stresses.

3.1. Cross-sectional analysis

In order to couple VABS with the YF model, the cross-sectional parameters in the YF strain energy formulation are replaced with their VABS counterparts. This implies that the Y_{ij} terms in Eqs. (36)–(40) are replaced with the corresponding right hand side terms. The warping cross-sectional properties, Y_{i8} and Y_{i9}, as well as Y_{27}, Y_{37}, and Y_{77} are set to zero since there are no VABS counterparts. The YF warping cross-sectional coefficients need to be set to zero in order to avoid "double counting" of the strain energy due to warping since VABS already accounts for warping in the **H**, **A**, **B**, **C**, and **D** matrices. Even

though strain energy contributions associated with Y_{27}, Y_{37}, Y_{77}, and $u^{(V)}_{\text{H.O.T.}}$ are not accounted for in the YF/VABS model, the YF/VABS formulation represents an accurate representation of the "actual" strain energy since the unaccounted for terms are higher order functions of the 1D strain measures than the terms which are accounted for. For example, Y_{27} is associated with the shear-twist coupling $\kappa_1^2\gamma_{12}$, which is higher order than the $\kappa_1\gamma_{12}$ term corresponding to H_{24}.

This process of replacing appropriate coefficients in the YF model with equivalent VABS parameters and setting various cross-sectional coefficients equal to zero will result in a "hybrid" strain energy formulation which will be different from $U^{(Y)}$ and $\widetilde{U}^{(V)}$. In certain regards, the YF/VABS hybrid strain energy will be more accurate for composite beam modeling than the original YF formulation based on the cross-sectional analysis from Kosmatka (1986) since in-plane stresses and warping are accounted for, and out-of-plane warping is treated in a more general manner by VABS. Furthermore, the loss in accuracy compared to the original YF and VABS strain energy formulations is due to the neglect of higher order terms, and thus is expected to be insignificant.

The YF/VABS kinetic energy cross-sectional parameters are taken directly from the VABS outputs for Eqs. (41)–(46) since the YF model requires these coefficients. The kinetic energy parameters associated with warping velocities are set to zero since VABS does not account for warping inertia. However, the kinetic energy contribution from warping is not expected to be significant. Therefore, since higher order strain energy terms and warping inertia are not considered to be significant, the differences between the two formulations do not prohibit coupling of VABS with the YF model.

3.2. Solution of 1D beam displacements

Using the VABS cross-sectional outputs as inputs to the YF model based on the procedure described above does not require modification of the 1D kinematics associated with the YF model. Thus, upgrading the cross-sectional analysis does not require significant modification to the rotorcraft analysis code since only the inputs to the blade model have been modified. This implies that the strain–displacement relations employed in Yuan and Friedmann (1995) are retained, and the 1D beam displacements – axial, bending, torsion, and shear deformation – are solved for by the finite element method utilized in the original YF model. Since the strain–displacement relations are based on the ordering scheme described in Yuan and Friedmann (1995), the YF/VABS model is only valid for moderate deflection analysis, which is sufficient for most helicopter rotor blade applications. Comprehensive rotorcraft codes are usually developed over extensive time periods (years), thus substantial modification of such codes is a complex and time consuming task. Therefore modifying the numerous subroutines associated with an existing complicated analysis code in order to incorporate a more general geometrically exact 1D kinematic formulation is not justified.

3.3. Recovery of cross-sectional warping displacements

Since Y_{i8} and Y_{i9} are set to zero in the YF/VABS model, the out-of-plane warping amplitude α is eliminated from the finite element discretized equations of motion. Therefore, warping must be calculated using the VABS warping recovery relations. The warping recovery relations approximate V_j as functions of γ_{11}, $2\gamma 12$, $2\gamma_{13}$, κ_1, κ_2, and κ_3 using the variational asymptotic approach (Hodges, 2006). In the YF/VABS model, warping displacements are obtained from the VABS warping recovery relations as follows:

(1) The beam 1D displacements are solved for using the finite element approach.
(2) The 1D strain measures are recovered by substituting the displacements into the YF strain–displacement relations.
(3) The 1D strain measures are substituted into the VABS warping recovery relations, which yield in and out-of-plane warping displacements.

It is worth noting that by eliminating the 1D variable α, the capability to model restrained warping, i.e. constraining warping displacements at the boundary to be zero, is lost. Without a 1D variable associated with warping, there is no way to enforce boundary conditions on the warping displacements at the root. However, accounting for restrained warping is generally not considered to be critical for composite closed cross-sections (Hodges, 2006; Volovoi et al., 2001), even though exceptions are known to exist (Rehfield et al., 1990). In the most extreme example presented by Rehfield et al. (1990), a moderate error of 11% was observed in the prediction of the tip twist deformation when neglecting restrained warping effects. Furthermore, the Vlasov-type approach to restrained warping available in VABS is only appropriate for open cross-sections and may produce errors if used for closed section modeling (e.g. Chapter 7 of Hodges, 2006), and therefore is not used with the YF/VABS model. Thus, the YF/VABS model is suitable for rotor blade analysis since helicopter rotor blades are modeled as closed cross-sections. Furthermore, accounting for restrained warping effects associated with closed sections would likely produce only moderate gains in accuracy at most.

3.4. Stress recovery

The YF/VABS strain field is recovered by substituting the 1D strain measures and cross-sectional warping derivatives into Eqs. (11)–(14). Note that the contributions from in-plane warping are included in the YF/VABS strain field since VABS

accounts for in-plane warping. Stresses are obtained by substituting Eqs. (11)–(14) into Eq. (16) instead of Eq. (19) since VABS accounts for in-plane stresses.

It should be noted that a higher order beam theory would be needed to impose zero beam strains at the root and therefore the current approach will only provide an accurate estimation of the cross-sectional stress distributions away from the boundary.

4. Results

In this section, results from the YF/VABS model are compared with experimental data and other analysis codes. The YF/VABS model was validated by considering displacements and stresses due to static loading, as well as hover and forward flight helicopter applications. As in Hodges et al. (2007) and Hodges and Yu (2007), the trapeze effect was treated by setting $A_{22} = H_{55} + H_{66}$ and all other elements of **A**, **B**, **C**, and **D** to zero for all results. This is consistent with the YF model, in which $Y_{17} = Y_{55} + Y_{66}$.

4.1. Displacements and stresses under static loading

The YF/VABS static analysis capability is validated by considering a prismatic composite cantilevered beam, loaded by a vertical tip force. The YF/VABS results were compared with experimental data from Minguet and Dugundji (1990) and results generated by NLABS (nonlinear active beam solver, Palacios and Cesnik, 2008), which is based on the geometrically exact kinematic formulation for which VABS was designed. Details on the experimental setup can be found in Minguet and Dugundji (1990) and Cesnik and Hodges (1997). The static displacement results in Fig. 3 correspond to two composite cross-sections: (1) a symmetric layup, $[45^\circ/0^\circ]_{3s}$ which exhibits bending-torsion coupling and (2) an anti-symmetric layup, $[20^\circ/-70^\circ/-70^\circ/20^\circ]_{2a}$ which exhibits extension-twist coupling. The YF/VABS model compares well with the experimental results and NLABS until the loading is large enough to cause deflections over 10% of the beam length. This is expected since the ordering scheme used to simplify the YF strain–displacement relation is based on the assumption that the maximum bending deflections are on the order of 10–20% of the beam's length (Yuan and Friedmann, 1995). These results demonstrate that the YF/VABS model is valid for moderate deflection analysis, while a geometrically exact formulation is necessary to accurately model large deflections.

Fig. 4 shows the axial stress distribution at the midspan section calculated by NLABS, YF/VABS, and a 3D finite element solution using the MSC.NASTRAN linear static solver for the symmetric layup and a tip force of 0.0044 N, which is well within the moderate deflection regime. The NASTRAN model contains over 2 million degrees of freedom and requires 25 GB of memory and 8 h of simulation time on a 3.2 GHz Xeon processor. By comparison, NLABS and YF/VABS require less than 1 min of simulation time. Fig. 4 illustrates that the cross-sectional stress distributions calculated by YF/VABS and NLABS yield similar agreement with the NASTRAN results for moderate deflection analysis.

4.2. Helicopter applications

The YF/VABS model was validated against other composite rotor blade analyses by considering the fundamental rotating natural frequencies, aeroelastic stability characteristics in hover, and vibratory hubloads in forward flight. The aerodynamic loads used to generate the results in Yuan and Friedmann (1995) are based upon a relatively simple quasi-steady, incompressible aerodynamic model combined with a uniform inflow assumption. These loads were applied to a four bladed hingeless rotor, thus the dominant frequency of the oscillatory hubloads is 4/rev.

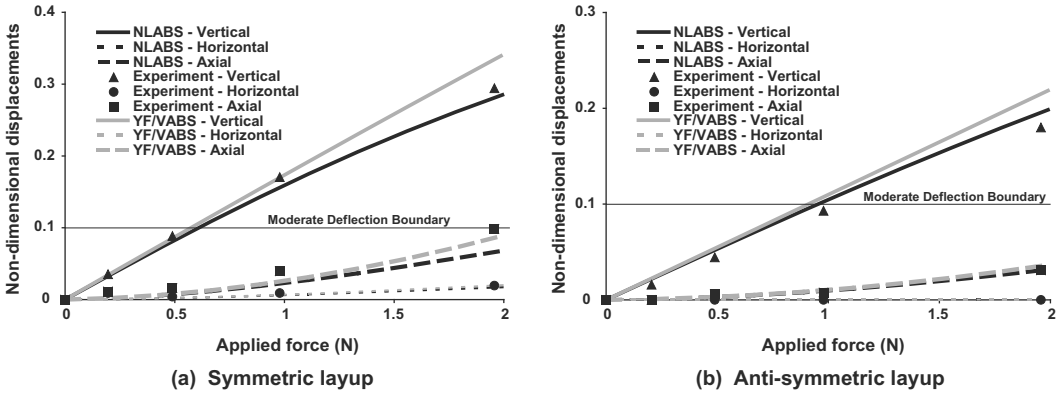

Fig. 3. Composite beam displacements, non-dimensionalized by the beam length.

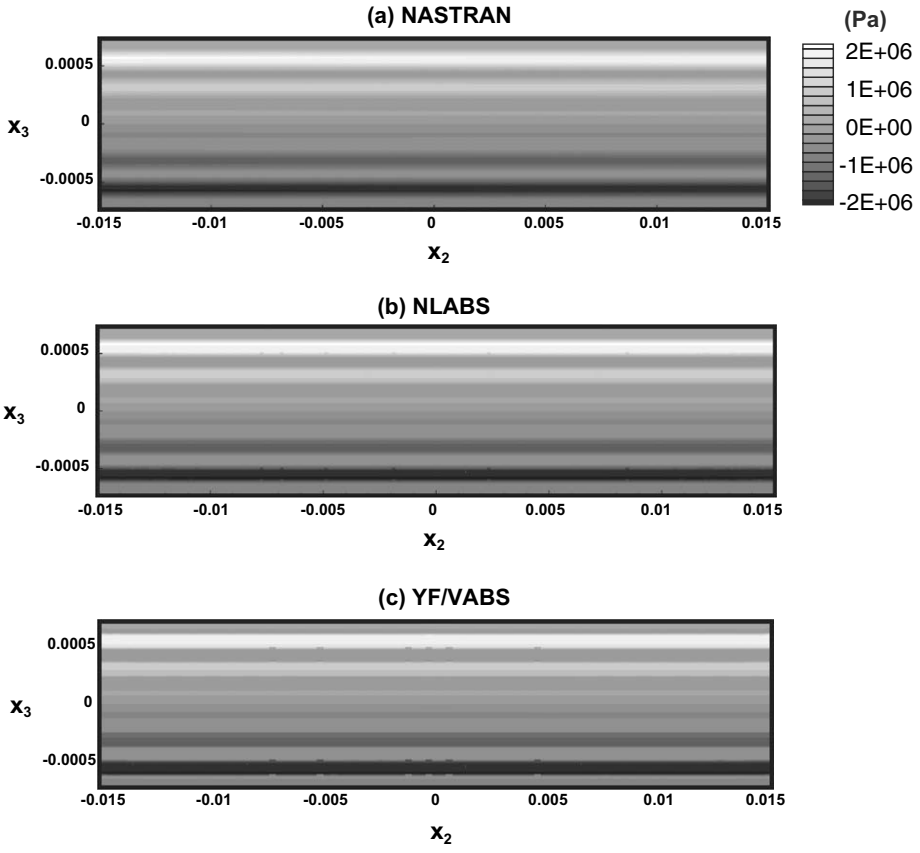

Fig. 4. Axial stress distributions (σ_{11}) corresponding to the symmetric layup.

4.2.1. Fundamental rotating natural frequencies of a single-cell composite blade

The single-cell composite rotor blade described in Friedmann et al. (2002) was considered in this study. In the single-cell section depicted in Fig. 5, the ply angles in the horizontal walls were set to zero while, Λ_v in both vertical walls was allowed to vary. As shown in Fig. 5, a positive Λ_v implies that the fibers are oriented toward the top of the blade.

For $\Lambda_v = 0$, the results presented in Table 1 display the differences between the fundamental rotating lead-lag, flap, and torsional natural frequencies – ω_{L1}, ω_{F1}, and ω_{T1} – calculated by the YF/VABS model, relative to the following analysis codes:

(1) Hong and Chopra (1985): The model employed in Hong and Chopra (1985) is based on a moderate deflection theory in which the transverse shear deformation was neglected. In-plane stresses and warping are neglected in the cross-sectional analysis.
(2) Fulton and Hodges (1993a,b): This model is based on a geometrically exact kinematical formulation and is valid for large deflection analysis. The cross-sectional analysis is based on Berdichevsky et al. (1992), and does not account for in-plane warping.
(3) Yuan and Friedmann (1995): This is the original moderate deflection YF model, which is based on the cross-sectional analysis described in Kosmatka (1986).

The results in Table 1 demonstrate good agreement between the fundamental frequencies predicted by YF/VABS and the other composite blade models. Note that the 3.4% difference between the torsional frequencies predicted by YF/VABS and the YF model can be attributed to the effects of restrained warping, which increase the torsional stiffness of the YF beam model.

4.2.2. Aeroelastic stability boundaries in hover

For aeroelastic stability in hover of a rotor blade, the governing equations of motion are linearized about a static equilibrium solution and cast into first-order state variable form (Friedmann et al., 2002). The eigenvalues of the linearized system determine the hover stability characteristics of the blade. A comparison of the real part of the first lead-lag eigenvalue for $\Lambda_v = -30^\circ, 0^\circ, 30^\circ$ as a function of thrust coefficient (C_T) divided by rotor solidity (σ) is given in Fig. 6 for the single-cell

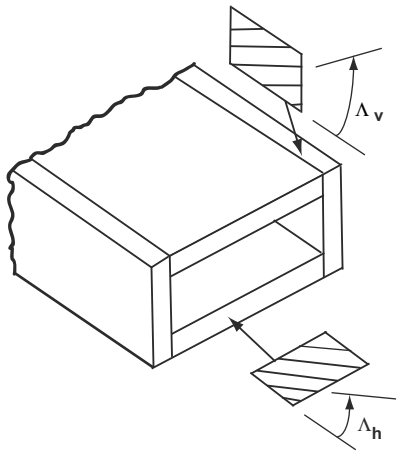

Fig. 5. Single-cell cross-section.

Table 1
Differences in YF/VABS fundamental frequencies relative to various models

Model	Percent differences		
	ω_{L1}	ω_{F1}	ω_{T1}
Hong and Chopra (1985)	1.5%	3.1%	0.2%
Fulton and Hodges (1993a,b)	5.0%	0.9%	−1.0%
Yuan and Friedmann (1995)	−0.7%	−0.5%	−3.4%

cross-section. The YF/VABS yields excellent agreement with the models by Fulton and Hodges (1993a,b) and Yuan and Friedmann (1995). In Friedmann et al. (2002), the poor agreement from Hong and Chopra (1985) with the other models for $\Lambda_v = -30^\circ$ and 30° was attributed to the neglect of transverse shear deformation.

Root locus plots of the hover stability eigenvalues as a function of ply angle Λ_v for the single-cell blade are shown in Fig. 7. Fig. 7 indicates that the YF/VABS model produces similar stability eigenvalues compared to the original YF analysis for each value of Λ_v. The differences between the YF/VABS and the original YF imaginary parts of the eigenvalues range from 0.1% to 3.8% relative to the YF values. The relative differences between the real parts range from 0.3% to 37%. The 37% relative difference, which corresponds to the lead-lag mode at $\Lambda_v = 30^\circ$ and $C_T = 0.0025$, is deceiving because the absolute difference is small, which is evident from Fig. 7(a). The relative error is large even though the absolute error is small because the YF/VABS and original YF models yield real parts of the lead-lag eigenvalue close to zero because the damping in the lag mode is very small for $\Lambda_v = 30^\circ$ and $C_T = 0.0025$. Excluding the lead-lag mode, there is a maximum relative difference of only 3.1% in the

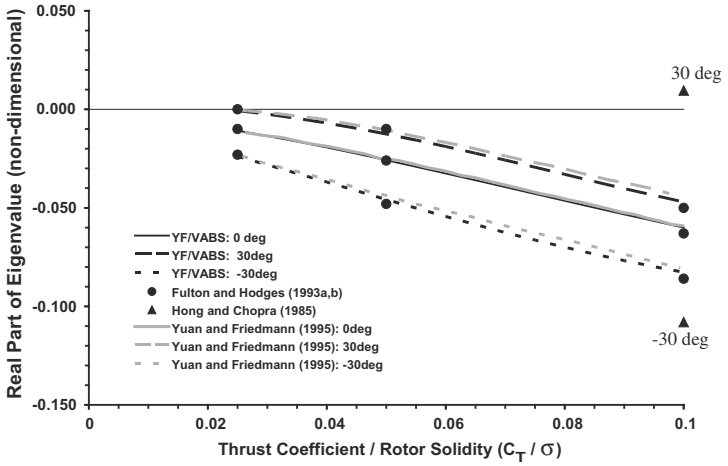

Fig. 6. Real part of the hover stability first lead-lag eigenvalue for the single-cell composite blade.

real parts of the eigenvalues. Therefore, there is strong agreement between YF/VABS and the original YF model for hover stability analysis of the single-cell composite blade.

In addition to the single-cell blade, hover stability of a double-cell composite blade with a cross-section depicted in Fig. 8 was considered. Details on the rotor and helicopter parameters can be found in Friedmann et al. (2002). For all cases considered in this study, the ply angles in the middle vertical wall and the inner half of the rear vertical wall were oriented at Λ_v, while ply angles in the remaining walls were set to zero.

The double-cell blade root locus eigenvalues are presented in Fig. 9. The maximum difference in the imaginary parts of the eigenvalues is less than 1%, while the differences between the real parts of the eigenvalues range from 2.2% to 11.4%. The differences due to the improved cross-sectional analysis in YF/VABS – i.e. accounting for in-plane warping and stresses, and a more general treatment of out-of-plane warping displacements even though restrained warping effects are neglected – lead to negligible differences in the imaginary parts of the hover stability eigenvalues, and less than 12% differences in the real parts for the double-cell blade. The results in Figs. 6–9 demonstrate that the hover stability analysis based on the YF/VABS model generally produces good agreement with other composite rotor blade analyses for the cross-sections considered in this study.

4.2.3. Vibratory hubloads in forward flight

Using the rotor and helicopter parameters from Yuan and Friedmann (1998), the 4/rev vibratory hub shears and moments were calculated for the double-cell composite blade at an advance ratio of 0.30. The vibratory hub shears and moments are obtained from the integration of the distributed inertial and aerodynamic loads over the entire blade span in the rotating frame. Subsequently, the loads are transformed to the hub-fixed non-rotating system, and the contributions from the individual blades are combined (Yuan and Friedmann, 1995). The vibratory hubloads calculated by YF/VABS are compared with the YF model in Fig. 10 for various values of Λ_v. It is clear from Fig. 10 that YF/VABS and the YF model predict similar trends in vibratory loads as Λ_v is varied. Furthermore, the differences in hub shears range from 0.1% to 8.7% relative to the YF values, and 0.01–8.2% for the hub moments. These results suggest that the VABS cross-sectional analysis will result in small to moderate differences in the vibratory loads compared to the model based on the cross-sectional analysis described in Kosmatka (1986).

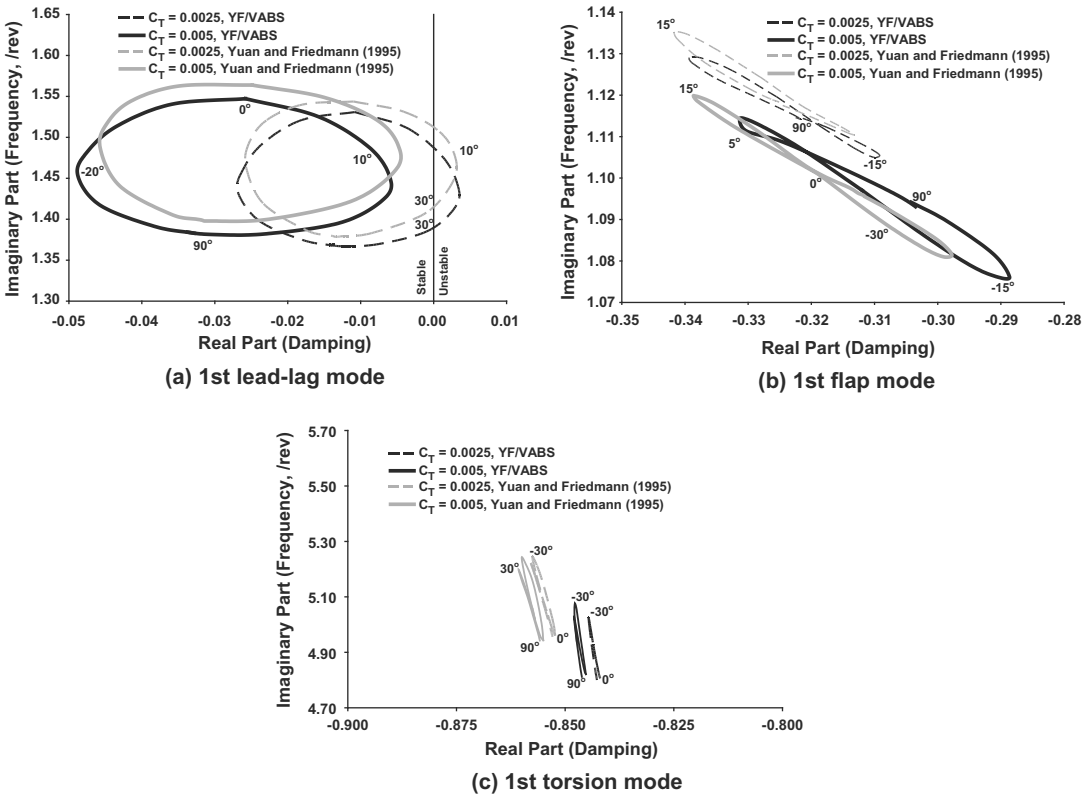

Fig. 7. Root locus eigenvalues as a function of Λ_v for the single-cell composite blade.

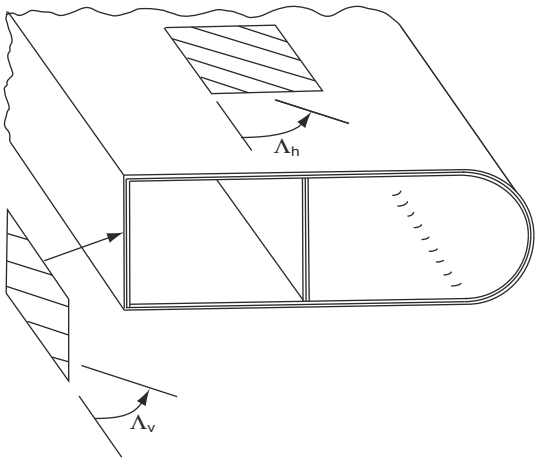

Fig. 8. Double-cell cross-section.

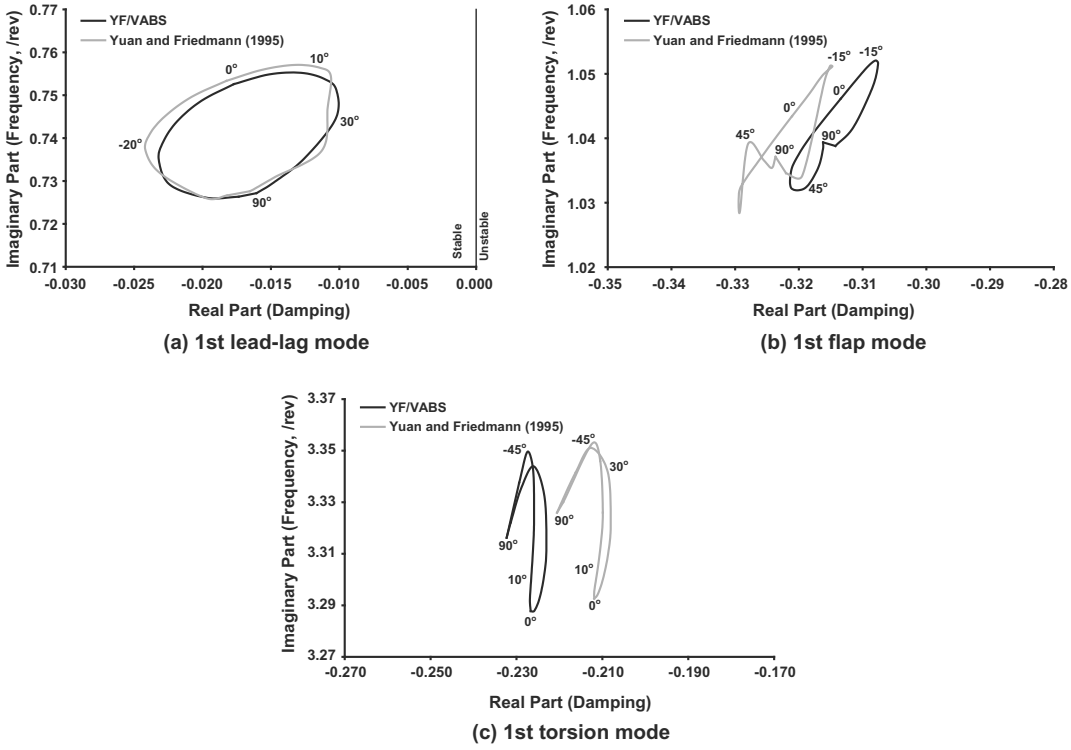

Fig. 9. Root locus eigenvalues as a function of Λ_v for the double-cell composite blade.

5. Conclusions

The results demonstrate that VABS is suitable for coupling with the moderate deflection composite blade model described in Yuan and Friedmann (1995), in spite of the differences between the formulations. Compared to the original YF blade model, YF/VABS will produce a more accurate stress field due to the more general treatment of warping. Furthermore, YF/VABS will produce accurate elastic stiffness quantities for composite cross-sections in which the neglect of in-plane stresses would result in large errors. The YF/VABS composite rotor blade model was validated against experimental data as well as other rotor blade analyses by considering static displacements and stresses, aeroelastic stability in hover for composite rotor

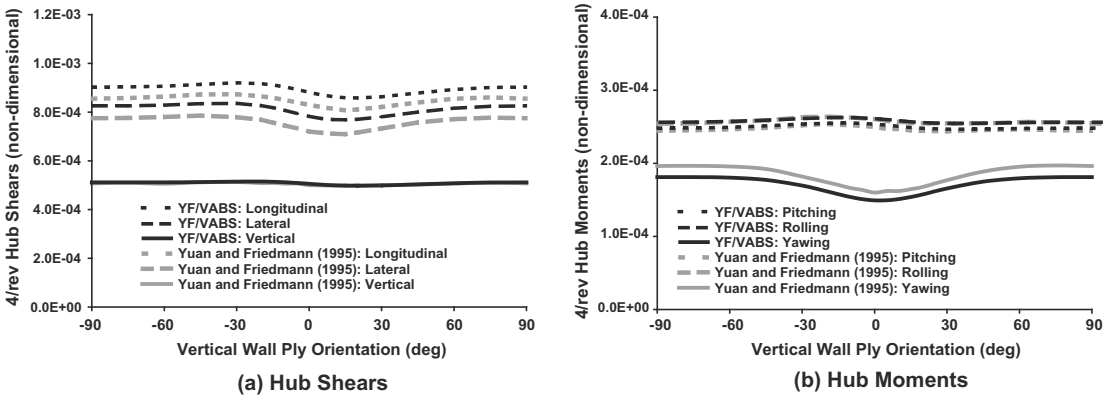

Fig. 10. Comparison of vibratory hubloads as a function of Λ_v.

blades, and forward flight vibratory hub shears and moments. Thus, this paper demonstrates the feasibility of combining a moderate deflection beam model with VABS. This finding facilitates the use of VABS in comprehensive rotorcraft simulation codes which employ a moderate deflection blade model. Thus, it has potential for improving the accuracy and versatility of such codes without requiring extensive investment of effort in code modification. The principal findings from this study are summarized below:

(1) The differences between the VABS and YF strain energy formulations are due to higher order effects, and thus do not preclude coupling between the two models.
(2) By using VABS with the YF blade model, the ability to account for restrained warping effects is lost. However, such effects generally are not critical for treating composite closed-cross sections, which is the type of structural configuration used for modeling composite rotor blades.
(3) For moderate deflections, YF/VABS compared well with a beam model based on geometrically exact kinematics and experimental displacement data corresponding to a composite beam under a static load. As expected, the geometrically exact NLABS model is superior to YF/VABS for large displacement analysis only, which is not expected to be critical for modeling well-designed helicopter blades.
(4) Fundamental rotating natural frequencies and hover stability eigenvalues calculated by YF/VABS correlated well with other composite rotor blade models for both single-cell and double-cell blade configurations.
(5) The vibratory hub shears in forward flight calculated by YF/VABS differed by 0.1–8.7% compared to the original YF values, and 0.01–8.2% for the hub moments. These results suggest that the VABS cross-sectional analysis will result in small to moderate differences in the vibratory loads compared to the cross-sectional analysis described in Kosmatka (1986).

Acknowledgements

This research was supported in part by a NASA Graduate Student Research Fellowship for B. Glaz with Dr. W. Warmbrodt as grant monitor. Partial support from the Center for Rotorcraft Innovation under WBS 2007-B-01-01.2-A17, as well as the Vertical Lift Research Center of Excellence (VLRCOE) sponsored by the NRTC with Dr. M. Rutkowski as grant monitor is also hereby acknowledged.

References

Berdichevsky, V.L., Armanios, E.A., Badir, A., 1992. Theory of anisotropic thin-walled closed-cross-section beams. Composites Engineering 2 (5–7), 411–432.
Bori, M., Merlini, T., 1986. A large displacement formulation for anisotropic beam analysis. Meccanica 21, 30–37.
Cardona, A., Geradin, M., 1988. A beam finite element non-linear theory with finite rotation. International Journal for Numerical Methods in Engineering 26, 2403–2438.
Cesnik, C.E.S., Hodges, D.H., 1997. VABS: a new concept for composite rotor blade cross-sectional modeling. Journal of the American Helicopter Society 42 (1), 27–38.
Crisfield, M.A., 1990. A consistent co-rotational formulation for non-linear, three-dimensional beam-elements. Computer Methods in Applied Mechanics and Engineering 81, 131–150.
Danielson, D.A., Hodges, D.H., 1987. Nonlinear beam kinematics by decomposition of the rotation tensor. Journal of Applied Mechanics 54, 258–262. June.
Friedmann, P.P., 2004. Rotary wing aeroelasticity – current status and future trends. AIAA Journal 42 (10), 1953–1972.
Friedmann, P.P., Hodges, D.H., 2003. Rotary wing aeroelasticity – a historical perspective. Journal of Aircraft 40 (6), 1019–1046.
Friedmann, P.P., Yuan, K.A., de Terlizzi, M., 2002. An aeroelastic model for composite rotor blades with straight and swept tips part I: aeroelastic stability in hover. International Journal of Non-Linear Mechanics 37, 967–986.
Fulton, M., Hodges, D.H., 1993a. Aeroelastic stability analysis of composite hingeless rotor blades in hover – part I: Theory. Mathematical and Computer Modelling 18 (3/4), 1–17.

Fulton, M., Hodges, D.H., 1993b. Aeroelastic stability analysis of composite hingeless rotor blades in hover – part II: Results. Mathematical and Computer Modelling 18 (3/4), 19–35.
Glaz, B., Friedmann, P.P., Liu, L., 2008a. Surrogate based optimization of helicopter rotor blades for vibration reduction in forward flight. Structural and Multidisciplinary Optimization 35 (4), 341–363.
Glaz, B., Friedmann, P.P., Liu, L., Jan. 2008b. Vibration and noise reduction of helicopter rotors using an active/passive approach. In: Proceedings of the American Helicopter Society Aeromechanics Specialists Conference, San Francisco, CA, pp. 1–18.
Hodges, D.H., 1990. Review of composite rotor blade modeling. AIAA Journal 28 (3), 561–565.
Hodges, D.H., 2006. Nonlinear Composite Beam Theory. AIAA, Reston, VA.
Hodges, D.H., Atilgan, A.R., Cesnik, C.E.S., Fulton, M.V., 1992. On a simplified strain energy function for geometrically nonlinear behavior of anisotropic beams. Composites Engineering 2, 513–526.
Hodges, D.H., Saberi, H., Ormiston, R.A., 2007. Development of non linear beam elements for rotorcraft comprehensive analyses. Journal of the American Helicopter Society 52 (1), 36–48.
Hodges, D.H., Yu, W., 2007. A rigorous, engineer-friendly approach for modeling realistic, composite rotor blades. Wind Energy 10, 179–193.
Hong, C.H., Chopra, I., 1985. Aeroelastic stability analysis of a composite rotor blade. Journal of the American Helicopter Society 30 (2), 57–67.
Ibrahimbegovic, A., Frey, F., Kozar, I., 1995. Computational aspects of vector-like parametrization of three-dimensional finite rotations. International Journal for Numerical Methods in Engineering 38 (21), 3653–3673.
Jung, S.N., Nagaraj, V.T., Chopra, I., 1999. Assessment of composite rotor blade modeling techniques. Journal of the American Helicopter Society 44 (3), 188–205.
Kosmatka, J.B., 1986. Structural dynamic modeling of advanced composite propellers by the finite element method. Ph.D. thesis, UCLA.
Minguet, P., Dugundji, J., 1990. Experiments and analysis for composite blades under large deflections, part I – static behavior. AIAA Journal 28 (9), 1573–1579.
Murugan, S., Ganguli, R., Harursampath, D., April 23–26, 2007. Effects of structural uncertainty on aeroelastic response of composite helicopter rotor. In: 48th AIAA/ASME/ASCE/AHS/ACS Structures, Structural Dynamics and Materials Conference. Honolulu, HI, pp. 1–18, AIAA Paper 2007-2298.
Myrtle, T.F., Friedmann, P.P., 2001. Application of a new compressible time domain aerodynamic model to vibration reduction in helicopters using an actively controlled flap. Journal of the American Helicopter Society 46 (1), 32–43.
Palacios, R., Cesnik, C.E.S., 2005. Cross-sectional analysis of non-homogeneous anisotropic active slender structures. AIAA Journal 43 (12), 2624–2638.
Palacios, R., Cesnik, C.E.S., 2008. A geometrically-nonlinear theory of active composite beams with deformable cross sections. AIAA Journal 46 (2), 439–450.
Patt, D., Liu, L., Friedmann, P.P., 2006. Simultaneous vibration and noise reduction in rotorcraft using aeroelastic simulation. Journal of the American Helicopter Society 51 (2), 127–140.
Popescu, B., Hodges, D.H., 1999. Asymptotic treatment of the trapeze effect in finite element cross-sectional analysis of composite beams. International Journal of Nonlinear Mechanics 34 (4), 709–721.
Rehfield, L.W., Atilgan, A.R., Hodges, D.H., 1990. Nonclassical behavior of thin-walled composite beams with closed cross sections. Journal of the American Helicopter Society 35 (2), 42–50.
Simo, J.C., 1985. A finite strain beam formulation the three-dimensional dynamic problem, part i. Computer Methods in Applied Mechanics and Engineering 49, 55–70.
Simo, J.C., Tarnow, N., Doblare, M., 1995. Non-linear dynamics of three-dimensional rods: exact energy and momentum conserving algorithms. International Journal for Numerical Methods in Engineering 38, 1431–1473.
Simo, J.C., Vu-Quoc, L., 1986. A three dimensional finite strain rod model, part ii: computational aspects. Computer Methods in Applied Mechanics and Engineering 58, 79–186.
Volovoi, V.V., Hodges, D., Cesnik, C.E.S., Popescu, B., 2001. Assessment of beam modeling methods for rotor blade applications. Mathematical and Computer Modelling. 33, 1099–1112 (April).
Yu, W., Hodges, D.H., Volovoi, V.V., Cesnik, C.E.S., 2002a. On timoshenko-like modeling of initially curved and twisted composite beams. International Journal of Solids and Structures. 39 (19), 5101–5121 (Sept.).
Yu, W., Volovoi, V.V., Hodges, D.H., Hong, X., 2002b. Validation of the variational asymptotic beam sectional analysis. AIAA Journal 40 (10), 2105–2112.
Yuan, K.A., Friedmann, P.P., May 1995. Aeroelasticity and Structural Optimization of Composite Helicopter Rotor Blades with Swept Tips. NASA CR 4665.
Yuan, K.A., Friedmann, P.P., 1998. Structural optimization for vibratory loads reduction of composite helicopter rotor blades with advanced geometry tips. Journal of the American Helicopter Society 43 (3), 246–256.